5-2-2018

Atomic Resolution X-Ray Crystal Structure of HIV-1 Protease in Complex with Atazanavir

Andrew N. Baumert
dbaumert1@student.gsu.edu

ATOMIC RESOLUTION X-RAY CRYSTAL STRUCTURE OF HIV-1 PROTEASE IN COMPLEX WITH ATAZANAVIR

by

ANDREW BAUMERT

Under the Direction of Irene Weber, PhD

ABSTRACT

Human immunodeficiency virus (HIV) is a pandemic that has infected nearly 1% of the world population. Despite numerous FDA approved antiviral drugs, HIV drug resistance remains a large challenge. HIV protease is an enzyme that is required by the virus to cleave Gag and Gag-Pol polyproteins into functional and structural proteins necessary for viral maturation. Currently, nine clinical inhibitors target HIV protease, but multiple clinical viral strains have developed resistance to these drugs. Therefore, it is necessary to continue developing new drugs to tackle the problem of HIV drug resistance, and X-ray crystallography is one tool that is used to study how drug candidates bind to HIV-1 protease. In order to study the interactions between inhibitor atazanavir and HIV-1 protease, the crystal structure of the complex has been solved at atomic resolution (1.09 Å). This structure will improve the design of new inhibitors for resistant protease.

INDEX WORDS: Crystallography, Human immunodeficiency virus, Structural biology

ATOMIC RESOLUTION X-RAY CRYSTAL STRUCTURE OF HIV-1 PROTEASE IN COMPLEX WITH ATAZANAVIR

by

ANDREW BAUMERT

A Thesis Submitted in Partial Fulfillment of the Requirements for the Degree of

Master of Science

in the College of Arts and Sciences

Georgia State University

2018

ATOMIC RESOLUTION X-RAY CRYSTAL STRUCTURE OF HIV-1 PROTEASE AND ATAZANAVIR

by

ANDREW BAUMERT

Committee Chair: Irene Weber

Committee: Donald Hamelberg

Kathryn Grant

Electronic Version Approved:

Office of Graduate Studies

College of Arts and Sciences

Georgia State University

May 2018

DEDICATION

This thesis is dedicated to Tyler Crawford and Rowan Feldhaus. Tyler, you played a big role in me deciding to attend Georgia State University, and I really wish that I was able to spend more time with you here. I will never forget the countless nights that we spent up together goofing off and talking about chemistry in undergrad. Rowan, changing our names was something that took an excruciating amount of time, and added a lot of stress to my first year at GSU. I'm extremely proud to have gone through the process with someone else, especially you. To both of you, thank you for pushing me to be myself, and teaching me to live life to the fullest. You have both shaped who I am as a person today, and for that I am eternally indebted to you.

ACKNOWLEDGEMENTS

I would like to thank Dr. Weber and everyone in her lab, Daniel Kneller, Andres Wong-Sam, Shelly Burnaman, Shrikant Pawar, Johnson Agniswamy and Yuan-Fang Wang, for taking me in. I would like to thank Johhny for helping me purify the protein and for collecting the X-ray data, and Yuan-Fang for helping me process the data and teaching me how to refine my structure. The X-ray diffraction data were collected at the Southeast Regional Collaborative Access Team (SER-CAT) beamline22ID at the Advanced Photon Source, Argonne National Laboratory. This research was supported by an NIH award, U10GM062920, under PIs Irene Weber and Robert Harrison.

Additionally, I would like to thank Dr. Renata Reis for teaching me about crystallography and providing me with encouragement, as well as my family for emotional support, interest in my work, and coming to visit me periodically.

TABLE OF CONTENTS

LIST OF TABLES

LIST OF FIGURES

LIST OF ABBREVIATIONS

AIDS – Acquired Immune Deficiency Syndrome

ATV – Atazanavir

AZT - Zidovudine

Cryo-EM - Cryo-Electron Microscopy

DRV - Darunavir

HAART – Highly Active Antiretroviral Therapy

HIV – Human Immunodeficiency Virus

HPLC – High Performance Liquid Chromatography

IN – Integrase

LB - Luria Bertani

mAU – milli Absorbance Units

NMR – Nuclear Magnetic Resonance

PDB – Protein Data Bank

PR – Protease

PR^{S17} - Highly Resistant Mutant of HIV-1 Protease Containing 17 Mutations

PR20 - Highly Resistant Mutant of HIV-1 Protease Containing 19 Mutations

RMSD - Root-mean-square deviation

RT – Reverse Transcriptase

SQV - Saquinavir

WT – Wild Type

1 INTRODUCTION

Human Immunodeficiency Virus (HIV) was transmitted to humans from non-human primates via cross-species transmission probably through hunting and butchering bushmeat and perhaps through capturing and trading primates and keeping them as pets.[1]

1.1 HIV Subtypes

Over 40 nonhuman primate species harbor species-specific simian immunodeficiency viruses. Independent cross-species transmissions have led to multiple HIV lineages. HIV-1 consists of groups M, N, O and P and HIV-2 groups A-H. HIV-1 group M is the primary source of the global HIV pandemic, and has infected over 33 million individuals, and HIV-1 group O has caused a few tens of thousands of infections primarily in West Africa. HIV-1 groups N and P have only been identified in a handful of individuals in Cameroon. HIV-1 groups M and N are believed to have originated from *Pan troglodytes troglodytes* in West Africa in independent cross-species transmission events, whereas HIV-1 groups O and P originated from *Gorilla gorilla gorilla* in Cameroon.[1]

1.2 Discovery of the Acquired Immune Deficiency Syndrome virus

In 1981, an editorial in *The New England Journal of Medicine* pointed out that scientists and doctors were puzzled by the fact that many men who sleep with men were suddenly contracting rare opportunistic bacterial, fungal and protozoan infections (including: *Mycobacterium pneumoniae, M. aviumintracellulare, Klebsiella pneumoniae, Candida albicans, Cryptococcus neoformans, Pneumocystis carinii, Toxoplasma gondii and Entamoeba histolytica)* and developing the rare Kaposi's sarcoma.[2] In 1983, two articles were published nearly simultaneously that identified the cause of this obscure immunodeficiency to be a retrovirus, later termed the human immunodeficiency virus.[3-4]

1.3 HIV replication cycle

HIV first infects its host using viral membrane-bound envelope (Env) glycoprotein trimers that bind to the host cell receptor and chemokine co-receptor, which is commonly CCR5 or CXCR4. The viral glycoprotein trimer consists of three heterodimers, each of which contains a noncovalently associated transmembrane glycoprotein gp41 and a surface glycoprotein gp120, which binds to the host cell receptor.[5-6] The viral and host membranes then fuse, and the contents of the viral particle are subsequently mixed with the host cells contents, including two single-stranded RNAs.[6]

Once inside the host cell, the viral RNA genome is reverse transcribed into DNA via the virus's reverse transcriptase (RT). RT contains two necessary functions in order to carry out this task: DNA polymerase activity, which can copy either a DNA or RNA template, and an RNase H, which degrades RNA only if it is forming an RNA-DNA duplex.[6-7] Next, the dsDNA is carried into the host cells nucleus and integrated into the host cell's chromosomes through integrase (IN), which acts as a multimeric complex.[8] The viral genome is then transcribed and translated using the host cells proteins. The resulting proteins are inactive *gag* and *gag-pol* polyproteins that must be further processed to produce mature viral particles; the *gag* polyprotein precursor contains matrix, capsid and p6 domains (as well as the spacers SP1 and SP2), and the *gag-pol* polyprotein precursor additionally contains the viral enzymes protease, reverse transcriptase and integrase.[9]

The virus then starts to assemble new viral particles inside of the host cell once the *gag* polyprotein has been translated and translocated to an assembly site.[9] Assembly occurs at the plasma membrane, where Env glycoproteins accumulate; the viral particle is released after *gag* recruits ESCRT, which drives the membrane scission reaction.[9]

Once the viral particles have been released from the host cell, the polyproteins must then be cleaved via HIV protease (PR) to form mature infectious viral particles.[9-10]

1.4 Historical and current HIV treatments

In the late 1980's, zidovudine (AZT) was the first antiretroviral agent to be approved for treatment of advanced HIV infection.[11-12] AZT is a nucleoside analog, which is converted to its active triphosphate form by various intracellular enzymes; once in its active form it binds to HIV-1 reverse transcriptase and prevents viral DNA synthesis.[11-12] For many years AZT was the only antiviral agent available for treatment of those with HIV and AIDS, and when given alone to patients with HIV, CD4 counts increased as well as general patient well being.[11-12] The infection still progressed to AIDS, and the life spans of patients with late-stage AIDS were mere months.[11-12] It was quickly realized that the benefits of AZT alone were short-lived, and AZT-resistant strains of HIV-1 were developing.[11]

1.4.1 Highly active antiretroviral therapy (HAART)

In the mid-1990's doctors began treating patients with HIV-1 with multiple antiviral agents with great success.[11, 13-15] Protease inhibitors were introduced in 1995, starting with saquinavir (SQV).[10] This treatment strategy, Highly Active Antiretroviral Therapy (HAART), was noted as a turning point in HIV treatment, with a dramatic decrease in HIV morbidity and life expectancy improvements.[16] HAART is a combination therapy that is comprised of at least three drugs from two different classes; typically one protease inhibitor or non-nucleoside reverse transcriptase inhibitor, combined with two nucleoside reverse transcriptase inhibitors.[11, 17] To date, there are antiviral agents that target different stages of the viral life cycle: cell entry and fusion, reverse transcription, integration, and maturation. While HAART clearly had many advantages, eventually it was uncovered that

it came with problems as well; HAART required patients to take upwards of 20 pills a day with very specific instructions, and missing even one dose a week could drastically increase the chance of the regimen failing.[11] Fortunately, HAART is capable of reducing viral load, improving immune function and increasing life expectancy.[17]

1.5 HIV protease

HIV PR is a member of the aspartic protease family, and cleaves specific sites in *gag* and *gag-pol* precursor polyproteins, and is essential for viral maturation.[18]

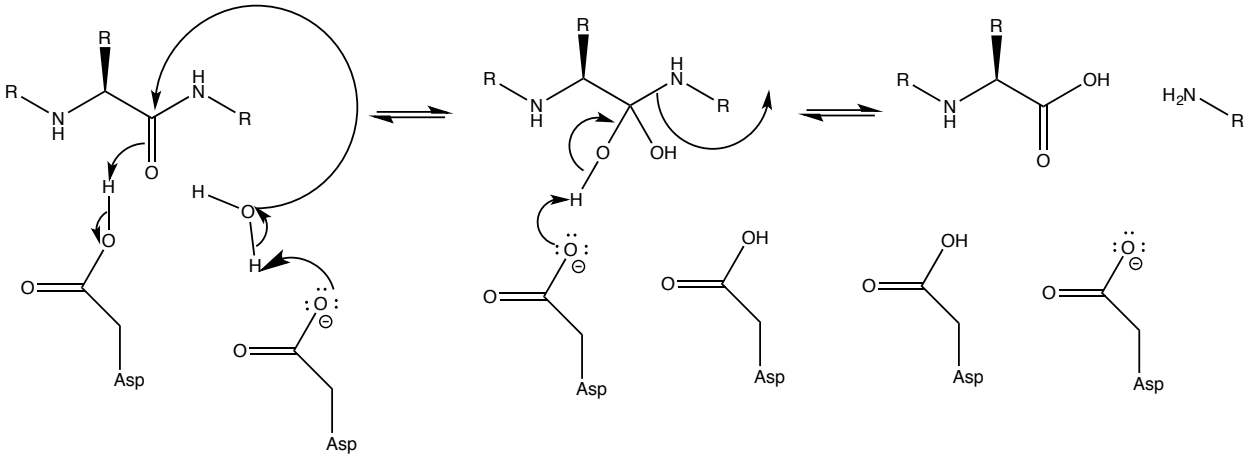

Figure 1.1 HIV protease mechanism, drawn in ChemDraw.

Rather than recognizing particular amino acid sequences, HIV PR works by recognizing the asymmetric shape of the peptide substrates; meaning that all of the cleavage sites have different sequences.[18] By inhibiting HIV PR, cell-to-cell transmission of the virus is stopped, because HIV PR is necessary for viral maturation.[19] HIV is able to mutate extremely rapidly because of reverse transcriptase lacks a proofreading function, and thus if the levels of antiviral drugs drop, then the development of drug resistance is likely.[11] Currently there are nine FDA approved protease inhibitors (PIs), and unfortunately, resistance mutations have been observed for each of these drugs.[18, 20]

1.5.1 General structure of HIV-1 protease

The active form of HIV-1 PR is a homodimer made of two 99 amino acid subunits, with the active site being along the dimer interface and each monomer contributing one of the two catalytic aspartates.[21] Two β-hairpins cover the active site, and act as highly flexible "flaps" that undergo large conformational changes upon binding and release of substrates and inhibitors.[22]

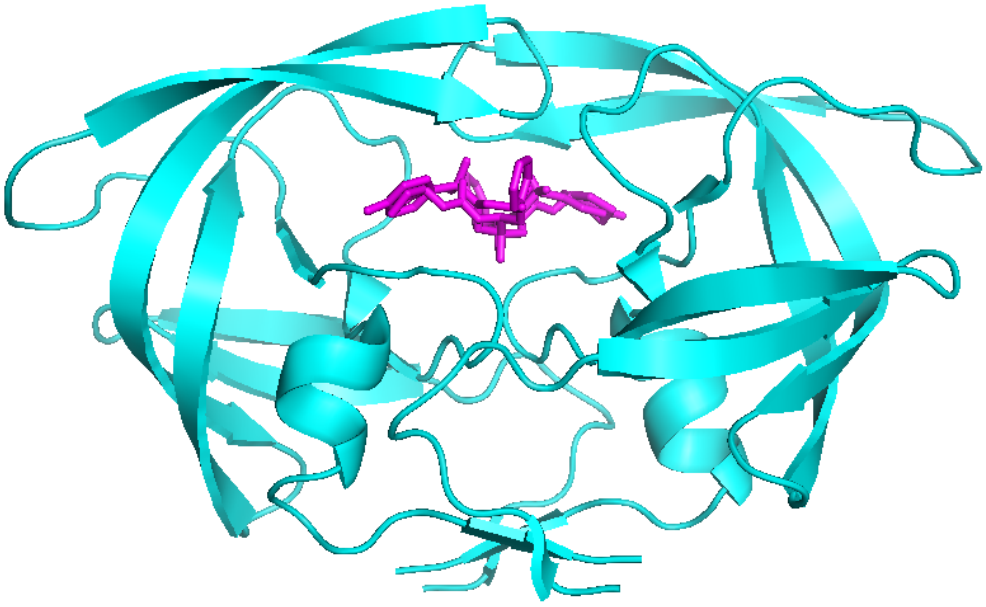

Figure 1.2 Crystal structure of HIV-1 PR in complex with amprenavir.

The crystal structure of 3NU3 is shown in Figure 1.2, modeled in PyMol.[23] The protease dimer is displayed as cyan ribbons and amprenavir as magenta sticks. The dimer is in a closed conformation when bound to substrate or inhibitor, and the flaps open away from the catalytic site to allow substrate or inhibitor to enter or be released.[10] In WT HIV-1 PR, three categories of flap conformations have been identified: closed, semi-open, and open.[24] In resistant mutants, flap dynamics are complex, and it is suggested that altered flap flexibility may contribute to drug resistance.[24]

1.5.2 Atazanavir

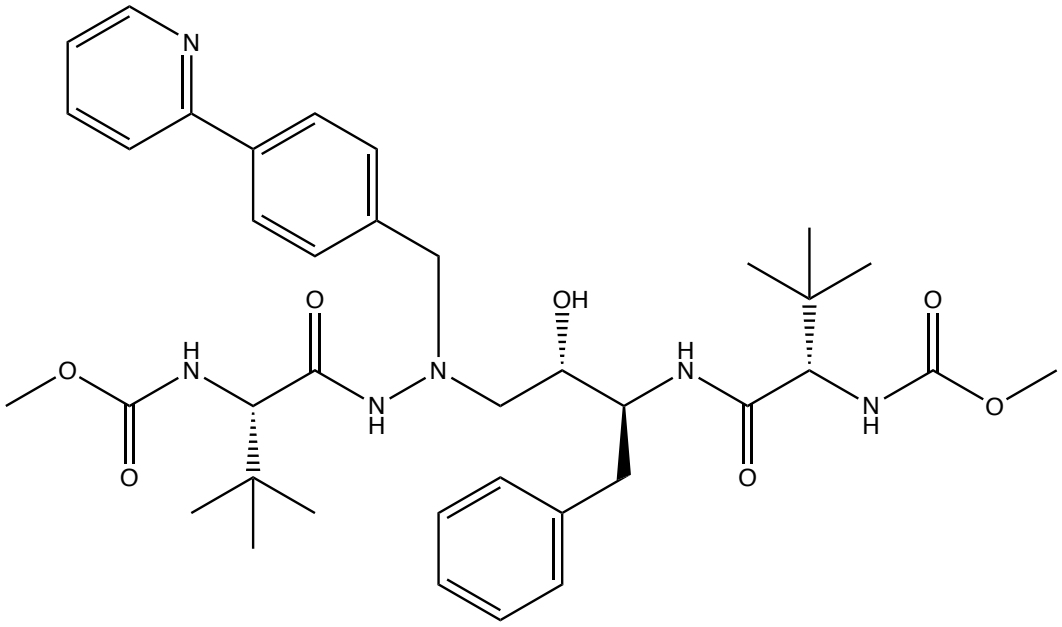

Figure 1.3. Structure of atazanavir, drawn with ChemDraw.

Atazanavir (ATV) is a peptidomimetic PI that has been approved in many countries for the treatment of adults with HIV-1 infection and in some countries, including the United States, children.[17] ATV is commonly used as a first-line therapy, and in some cases, ATV is administered with a boosting agent, ritonavir, and it is typically administered once daily.[17, 25] Like other PIs, ATV inhibits the cleavage of *gag* and *gag-pol* polyproteins, a step that must occur in an ordered fashion, and is essential for viral replication.[17, 20] ATV resistance profiles have been shown to be distinct from other PIs, and a signature resistance mutation has been identified as I50L, which was present in 100% of ATV resistant clinical isolates of patients not responding to ATV treatment.[17-18] In addition to I50L, the most common mutations that have co-emerged for patients using ATV +/- ritonavir include L10I/F/V/C, G16E, K20R/M/I/T/V, V32I, L33I/F/V, E34Q, M36I/L/V, M46I/L, G48V, F53L/Y, I54L/V/M/T/A, D60E, I62V, I64L/M/V, A71V/I/T/L, G73C/S/T/A, V82A/T/F/I,

I84V, I85V, N88S, L90M, and I93L/M.[17, 26] Mutations that are specific to patients using ATV (+/- ritonavir) are L10C, G16E, K20I/T/V, L33I/V, E34Q, F53Y, D60E, I64L/M/V, A71I/L, G73C/T, V82I, I85V, and I93L/M.[26]

1.6 HIV-1 protease and drug resistance

The RT used by HIV-1 during replication has notoriously low fidelity and lacks the ability to proofread, with typical retroviral RT error rates thought to be 10^{-4} to 10^{-6} errors per nucleotide, and is thus thought to be mostly responsible for the virus's rapid rate of mutation.[7, 27] Similar to other RNA viruses, HIV is faced with dynamic environments and thus must be a master of adaptation, though because of this, it must be careful also not to acquire too many mutations that lower viral fitness and push it towards extinction.[27] RNA viruses, like HIV, commonly exist as quasi-species, with enormous genetic diversity, which consequently allows them to escape control rapidly by antiretroviral drugs.[7, 28] In addition, the long-term nature of HAART often results in loss of adherence to the drug program and allows for the selection of resistant strains.[10] Resistance to PIs is caused by mutations in HIV-1 PR that either alter the inhibitor binding site or the dimer interface, while simultaneously retaining the ability to process Gag and Gag-Pol polyproteins.[10] In addition, Gag cleavage site mutations have also been observed that contribute to resistance.[25] HIV-1 PR is more susceptible to mutations than any other target of HAART, and multiple resistance mutations can be acquired, leading to highly resistant variants.[10, 25] "Major" resistance mutations of HIV-1 PR decrease binding of PIs, as well as natural substrates, which leads to reduced viral replication. "Minor" mutations can improve replication in viruses that contain "major mutations".[29]

1.7 Highly resistant HIV-1 protease variants

Despite the two newest PIs, darunavir (DRV) and tipranavir, being specifically designed to be effective against resistant mutants, PRs that are highly resistant to DRV and other PIs have been clinically isolated, leading to an interest in developing strategies to successfully inhibit resistant HIV PRs.[10] Many possible combinations of mutations in HIV PR are possible and highly resistant mutants frequently have 20 or more mutations, with the mutations likely acting synergistically in order to evade inhibitors in different fashions.[10, 24, 30]

1.7.1 Highly resistant mutant containing 20 mutations (PR20)

A clinically isolated highly resistant mutant of HIV-1 PR containing 19 mutations (PR20) retains its ability to process Gag and Gag-Pol polyproteins, even in the presence of current clinical protease inhibitors, although it processes the Gag polyprotein ~4 times slower than WT HIV-1 PR while maintaining the same order of cleavage.[24, 29, 31] PR20 contains 15 mutations that are classified as either major or minor drug resistance mutations.[32] Additionally, PR20 contains three major mutations associated with DRV resistance and has an 8,000-fold weaker binding affinity for DRV compared to WT HIV-1 PR.[30] PR20 exhibits a k_{cat} similar to that of wild-type (WT) PR, and PR20 also exhibits a K_m for a synthetic substrate that is ~13-fold higher relative to WT HIV-1 PR.[29] Additionally, PR20 exhibits a dimer dissociation constant (K_d) that is ~3 fold higher than that of WT HIV-1 PR, and uninhibited PR20 exhibits a thermal stability significantly greater than WT HIV-1 PR, being that PR20's T_m is 6°C higher than WT HIV-1 PR.[29] Inhibition of autoprocessing of a 56 amino acid transframe region is not observed for PR20, even in the presence of DRV and SQV that exceeds estimated plasma or intracellular concentrations.[29]

With all of these observations in mind, it is likely that PR20 is clinically unresponsive to all current PIs.[29] To date, the crystal structures of PR20 without inhibitor, as well as PR20 in complex with DRV and SQV, have been solved by the Weber lab.[29] By comparing the crystal structures of PR20 and WT HIV-1 PR, evolving mechanisms of drug resistance can be revealed, and strategies for targeting multidrug resistance mutants can potentially be improved.[29]

1.7.2 Highly resistant mutant containing 15 mutations (PR17)

PR^{S17} is another rationally selected clinically isolated highly resistant mutant of HIV-1 PR that is currently being studied in the Weber lab and contains six mutations in common with PR20.[30, 33] PR^{S17} retains its ability to autoprocess, and despite only containing one mutation in the substrate-binding cavity, PR^{S17} is resistant to all clinical inhibitors.[30, 33] The mutations of PR^{S17} are found in clusters and lack direct interactions with inhibitors.[30] Additionally, despite lacking all of the major mutations associated with DRV resistance, PR^{S17} has a binding affinity for DRV that is 10,000 fold weaker than WT HIV-1 PR, suggesting the basis of drug resistance may differ between PR20 and PR^{S17}.[30] PR^{S17} exhibits a low K_{dimer}, comparable to WT HIV-1 PR.[33] Structural studies of PR^{S17} in complex with DRV revealed that only two G48V and V82S, have contact with DRV, and the complex exhibits the closed flap conformation.[30] PR^{S17} in complex with DRV, compared to WT HIV-1 PR, exhibits a large conformational change in the hinge loop region (residues 34-42), which leads to a loss in the ion pair between E35 and R57 observed in WT HIV-1 PR.[30] It is possible that PR^{S17} represents a common mechanism of drug resistance, and thus it could be a representative model to design inhibitors for drug resistant mutants whose resistance is due to distal mutations.[30]

2 X-RAY CRYSTALLOGRAPHY AND DRUG DESIGN

2.1 Current techniques in structural biology

Current techniques in structural biology include cryo-electron microscopy (cryo-EM), nuclear magnetic resonance (NMR), neutron crystallography, and X-ray crystallography.[34-36] Cryo-EM is a technique that allows for structure determination with near-atomic resolution (~3.5Å) and does not require crystallization, which poses a major bottleneck in crystallography techniques.[34, 37] However, using cryo-EM for determining the structure of smaller and dynamic samples remains a significant challenge.[37] NMR is especially useful in studying protein dynamics, however it has intrinsic low sensitivity and thus requires large amounts of protein.[38] While there have been recent advancements in protein NMR methods; it is typically quite difficult to study large proteins, or those with a mass above 30 kDa.[38] Despite a few fundamental limitations (protein crystallization, unresolved dynamics, and limited detection of chemical heterogeneity), X-ray crystallography has remained the primary method of 3-D structure determination of proteins, viruses and nucleic acids, and structures determined by X-ray crystallography continue to be the majority of structures deposited in the PDB.[34, 39]

2.2 Why use X-ray crystallography?

X-ray crystallography is the central experimental technique used in structure-assisted drug design because structure solution and refinement are becoming increasingly more automated and newer synchrotrons allow for diffraction data to be collected rapidly and with high resolution from small crystals.[34, 36, 38] Furthermore, resolution of the diffraction data for a structure is an important parameter to consider, especially when using a structure for drug-design, because the atomic coordinates of a 1.5 Å structure are much more reliable than that of a structure with 3.5 Å resolution.[40] Unfortunately, structures in the PDB may contain errors, which can be problematic

for structure-guided drug design, specifically with structures that contain errors in the modeling of ligands in protein-ligand complexes.[34]

2.3 Structure-guided drug design and HIV-1 PR

Structure-guided drug design uses structure determination techniques (such as X-ray crystallography or NMR) and computational biology to guide the synthesis of drugs.[41] Structural studies of HIV-1 PR in complex with various inhibitors have been important in drug design; however, they have also historically been complemented with computational studies, such as docking and molecular dynamics, to understand the mode of inhibitor binding, and for optimization of inhibitor design.[41] Inhibitors of HIV-1 PR have been designed to maximize interactions with the enzymes backbone in the active site, which has led to potent FDA approved inhibitors with high barriers to resistance.[42] Analysis of crystal structures of WT HIV-1 PR in complex with DRV, as well as mutant PRs, have shown extensive hydrogen bonding between the PR backbone and inhibitor.[42] This suggests that designing inhibitors with increased interactions with the WT HIV-1 PR backbone will likely retain potency against mutant strains due to their lack of the ability to eliminate inhibitor-backbone interactions.[42]

2.3.1 The importance of atomic resolution

X-ray crystal structures can potentially reveal the locations of H atoms typically around 1 Å resolution, which is extremely important in structure-guided drug design, because H atoms play critical roles in H-bonding, electrostatic interactions and catalysis.[35, 42]

2.4 Protein crystallization

To solve the crystal structure of a protein (or DNA, small molecule, etc.), first a crystal must be formed. To achieve this a solution of protein is manipulated to induce supersaturation of the protein to produce protein crystals. There are three main methods to produce crystals: vapor-

diffusion, liquid-diffusion and batch, however for this work only vapor-diffusion was used. Vapor-diffusion can be further divided into hanging-drop and sitting-drop methods. In vapor-diffusion methods, a protein solution is mixed with a reservoir solution to form a small drop, which is typically just a few μL, and the drop is placed on a surface. The droplet is then sealed inside an airtight chamber, along with the reservoir solution. The droplet and the reservoir solution undergo a dynamic equilibration until the drop and the reservoir together reach a state of equilibrium.

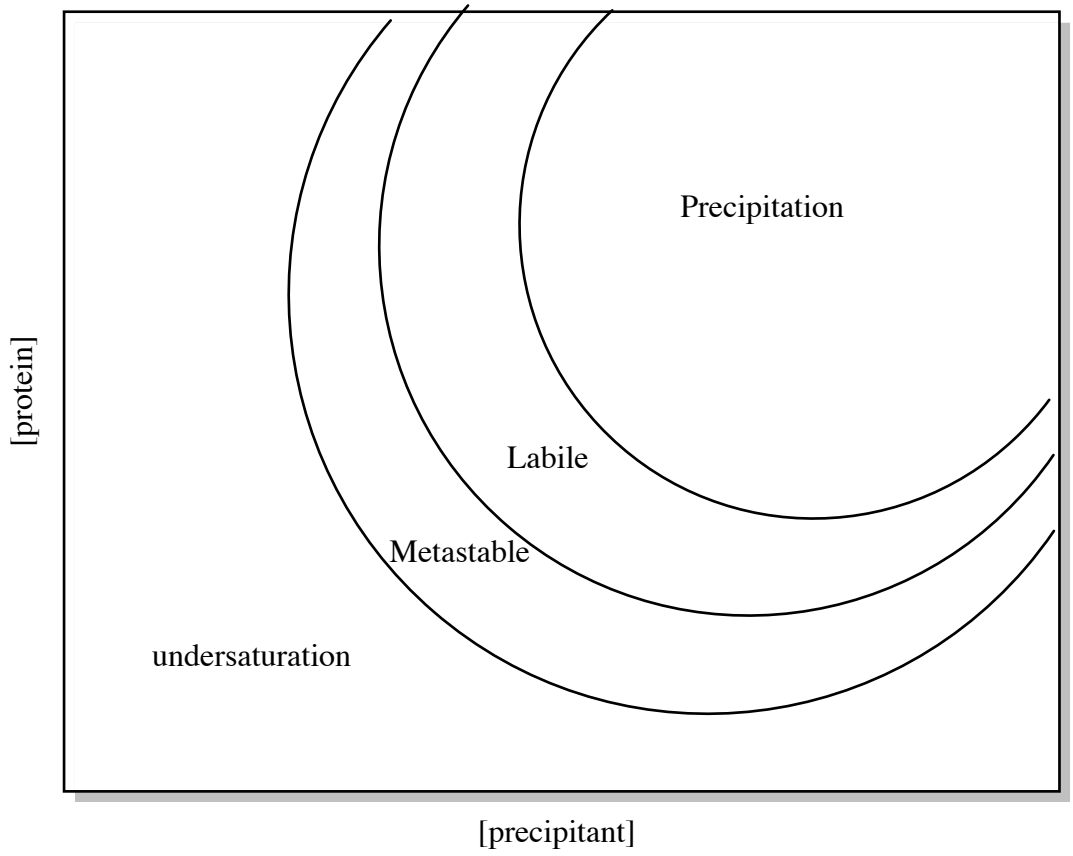

Figure 2.1 Simplified phase diagram for crystallization of proteins, created in ChemDraw.

The goal is for the protein to exceed its solubility limit, in the metastable zone, and not precipitate, but instead form crystals.[43] There is no way to predict what conditions will achieve

this goal, but fortunately there are many kits that assess a wide array of crystallization conditions, assisting one in determining what conditions to start with.[39, 43]

2.5 X-ray diffraction, data processing and refinement

Once crystallization conditions have been optimized to produce crystals that are seemingly worthy of diffraction, the crystal is fished into a loop and frozen, and then X-ray data can be collected using either a home source, or an X-ray beam generated by a synchrotron.[44] Typically, a synchrotron is preferred over a home source, due to the higher quality of data that it can yield.[44] During data collection, the crystal is rotated, and many frames of diffracted X-rays are collected on a detector.[45] Each reflection provided on the diffraction map is characterized both by its amplitude and phase; the peak intensities can provide amplitudes, but the reflection does not provide any direct information about the phase.[39] The phase of light cannot be directly measured, so to solve the structure, the phase problem must be addressed.[45] While there are a few ways to approach the phase problem, in the case of HIV-1 protease, many high-quality structures are available, so the molecular replacement method can easily be employed to solve this problem (in fact, this method has been used for nearly 80% of structures deposited in the PDB).[39, 46] Once the phase problem has been addressed an electron density map can be produced, which can then be refined (varying model parameters to achieve similarity between observed and calculated reflection amplitudes) and fit to solve the crystal structure.[47]

2.6 Currently available structures of HIV-1 PR and ATV complex

Prior to this study, there were three structures of other groups' HIV-1 PRs in complex with ATV available in the protein data bank (PDB), however these structures are considered to have moderate resolution (Table 1) compared to what has been recently achievable with HIV-1 PR in the Weber lab, and the WT sequences are not identical (Figure 2.2) to that of the Weber lab.[48-49]

Additionally, the three current structures have differences between the conformation(s) of ATV. It is important to note that proteases studied in the Weber lab have optimizing mutations, Q7K, L33I, and L63I, to increase protein stability and C67A and C95A to prevent the formation of disulfide bonds.[23] Other sequences differences are presumed to be polymorphisms.

PDB ID	Resolution (Å)	Space group	R_{free}	R_{work}
2AQU	2.0	$P6_1$	0.238	0.227
3EKY	1.8	$P2_12_12_1$	0.209	0.176
3EL1	1.7	$P2_12_12_1$	0.205	Not provided

Table 1. Crystallographic data for crystal structures of WT HIV-1 PR available in PDB.

```
WEBERWT:        PQITLWKRPLVTIKIGGQLKEALLDTGADDTVIEEMSLPGRWKPKMIGGIGGFIKVRQYD
2AQU:           PQITLWQRPLVTIKIGGQLKEALLDTGADDTVLEEMSLPGRWKPKMIGGIGGFIKVRQYD
3EKY:           PQITLWKRPLVTIRIGGQLKEALLDTGADDTVLEEMNLPGKWKPKMIGGIGGFIKVRQYD
3EL1:           PQITLWKRPLVTIRIGGQLKEALLDTGADDTVLEEMNLPGKWKPKMIGGIGGFIKVRQYD
                ******:******.******************:***.***.********************

WEBERWT:        QIIIEIAGHKAIGTVLVGPTPVNIIGRNLLTQIGATLNF
2AQU:           QILIEICGHKAIGTVLVGPTPVNIIGRNLLTQIGCTLNF
3EKY:           QIPIEICGHKAIGTVLVGPTPVNIIGRNLLTQIGCTLNF
3EL1:           QIPVEICGHKAIGTVLVGPTPVNIIGRNLLTQIGCTLNF
                ** :**.****************************.****
```

Figure 2.2 Multiple sequence alignment of sequences from other WT HIV-1 PR structures currently available in the PDB.

2.7 Benefits of protease – inhibitor atomic resolution structures

By solving an atomic resolution structure of WT HIV-1 PR in complex with ATV, more accurate comparisons of drugs interacting with WT HIV-1 PR can be made between ATV and DRV. Additionally, the interactions between ATV and highly drug resistant mutants can be compared with interactions in WT HIV-1 PR. By comparing these interactions in both WT and highly drug resistant mutants, more insight can be provided into designing drugs that are more potent against highly drug resistant mutants.

3 EXPERIMENT

Using *Escherichia coli* cells, HIV-1 protease was expressed in inclusion bodies, which were cleaned and HIV-1 PR was purified using gel filtration chromatography and high performance liquid chromatography. The PR was then dialyzed and refolded. The pure protein was then used to produce crystals in complex with ATV, and X-ray diffraction patterns were collected at a synchrotron, and the data was used to solve the structure of WT HIV-1 PR in complex with ATV structure with 1.09 Å resolution.

3.1 Purification of HIV-1 Protease

3.1.1 HIV-1 protease overexpression

Using BL21(DE3) cells harboring a plasmid containing the gene for HIV-1 PR, a 100 mL culture of pre-innoculum cells was grown in Luria Bertani (LB) broth containing 100 mg/ml carbenicillin. 10 mL of pre-innoculum was used to inoculate four 1 L flasks of LB broth containing 100 mg/mL carbenicillin. The cultures were grown at 37°C at 200 rpm to an OD of 0.6-0.8 when they were then induced with a final concentration of 2 mM isopropyl β-D-1-thiogalactopyranoside. The cultures were grown for 4 hours after induction and were then centrifuged at 5,000 rpm for 20 minutes at 4°C. The cells pellets were then stored at -80°C until further use.

3.1.2 HIV-1 protease inclusion body processing

The pellets were homogenized in 20 mL/1g cell pellet sonication buffer (50 mM tris pH 8.0, 10 mM EDTA pH 8.0, 1 mg/mL Lysozyme). 200 μL Triton-X 100 was added per 20 mL sonication buffer, and the cells were stirred for 2 hours. The cells were then sonicated on ice six times for 1 minute with 2 minute breaks. The cells were then centrifuged at 12,000 rpm 4°C for 20 min, the supernatant was discarded, and the pellet was resuspended in buffer B (50

mM tris mM, 10 mM EDTA pH 8.0, 2 M urea). The cells were then centrifuged again at 12,000 rpm, 4°C for 20 minutes and the pellet was resuspended again in buffer B. The cells were then centrifuged again at 12,000 rpm, 4°C for 20 minutes and the pellet was resuspended in buffer A (50 mM tris pH 8.0, and 20 mM EDTA pH 8.0). The cells were then centrifuged again at 12,000 rpm, 4°C for minutes. The pellet was resuspended in 10 mM DTT and stored at -20°C until further use.

3.1.3 Gel Filtration Chromatography

HiLoad™ 26/600 Superdex™ 75 pg size exclusion column was washed with two column volumes of degassed deionized water, and again with two column volumes of gel filtration buffer (3 M guanidine HCl, 50 mM Tris pH 8.0, 5 mM EDTA pH 8.0, 5 mM DTT). The inclusion bodies were thawed in a water bath and centrifuged at 12,000 rpm for 20 minutes at 4°C. The pellet was resuspended in 8 M guanidine HCl, 10 mM DTT and mixed for 1 hour. The solution was then filtered with a 0.8 micron filter. The sample was then injected into the column and run with a flow rate of 2.000 mL/min. The HIV-1 PR peak was collected and pooled and stored at -20°C for further use.

3.1.4 High-Performance Liquid Chromatography

HPLC column was equilibrated with two column volumes of 0.05% trifluoroacetic acid. The HPLC column was loaded with 5 mL gel filtration fractions and run with a flow rate of 1.000 mL/min. The protease eluted at 30% acetonitrile/70% water/0.05% trifluoroacetic acid. The HIV-1 PR peak was collected and pooled and stored at -20°C for further use.

3.1.5 Dialysis and refolding

The HPLC fractions were injected into a Slide-A-Lyzer™ dialysis cassette and incubated in 2 L 25 mM formic acid/1 mM DTT overnight at 4°C. The cassette was then transferred to 50

mM sodium acetate pH 5.0 at 4 °C for 4 hours. The protein was then concentrated by centrifugation, and the protein concentration was determined by absorbance at 280 nm.

3.2 Crystallization of HIV-1 protease in complex with atazanavir

3.2.1 Initial crystallization screening

Crystallographic conditions were screened using Hampton Research Crystal Screen™ HR2-112 kit and the hanging drop vapor diffusion method. The crystallization drops consisted of 1 μL of 4.2 mg/mL HIV-1 PR/2mM ATV and 1 μL reservoir solution.

3.2.2 Crystallization for X-ray diffraction

Four of the most promising conditions from the screening kit that produced crystals were further explored. Optimization involved varying concentrations of the screening reagents and the pH of the buffers. The HIV-1 PR and ATV concentration, temperature and hanging drop vapor diffusion method remained the same.

3.3 X-ray Data Collection and Structure Refinement

X-ray diffraction data was collected on ID beamline of the Southeast Regional Collaborative Access Team (SER-CAT) at the Advanced Photon Source at Argonne National Laboratory. The diffraction data was scaled and integrated with HKL2000, and the HIV-1 PR in complex with ATV structure was solved by molecular replacement with the HIV-1 PR in complex with amprenavir (3NU3) as the starting model by PHASER and CCP4.[50-52] The structure was refined using SHELX-2014 and model building was carried out using *Coot*, and anisotropic B factor refinement was applied.[53-54]

4 RESULTS

HIV-1 protease was purified from inclusion bodies using gel filtration chromatography and high-performance liquid chromatography and was dialyzed, refolded and concentrated. The protease was then crystallized using hanging drop vapor diffusion, and X-ray diffraction patterns were collected for numerous crystals. The highest quality diffraction data was used to solve the HIV-1 in complex with ATV by molecular replacement, using 3NU3 as a model.

4.1 HIV protease purification

4.1.1 Gel filtration chromatography of HIV protease

HIV-1 protease inclusion bodies were washed and dissolved in 5 mL 8 M guanidine HCl 10 mM DTT and injected into the gel filtration column and ran with a flow rate of 2.000 mL/min. The protein eluted in fractions 24-34 (Figure 4.1) and had a λ_{max280} = 200 mAU. In Figure 4.1, the x-axis represents mL, and the y-axis represents mAU.

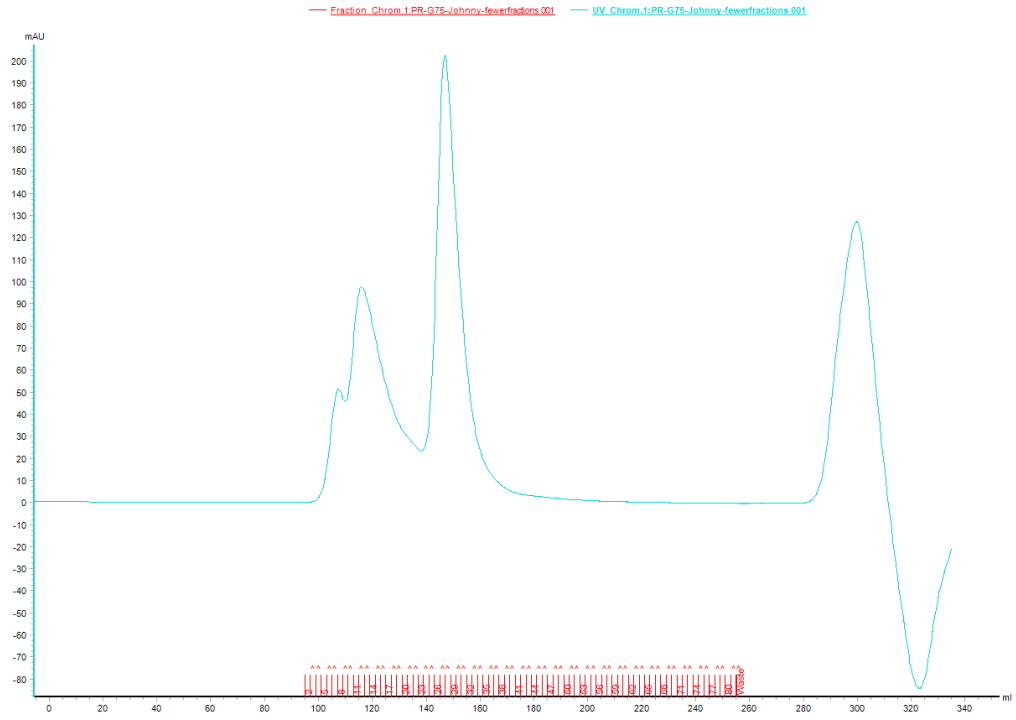

Figure 4.1 Gel filtration chromatogram of HIV protease.

4.1.2 HPLC of HIV protease

The resulting protein fractions from gel filtration chromatography were pooled and injected into the HPLC, which was run with a flow rate of 1.000 mL/min. The protease eluted at 30% acetonitrile/70% water/0.05% trifluoroacetic acid in fractions 10 – 15 (Figure 4.2) and the protein peaks had a λ_{max280} = 290 mAU. In Figure 4.2, the x-axis represents mL and the y-axis represents mAU.

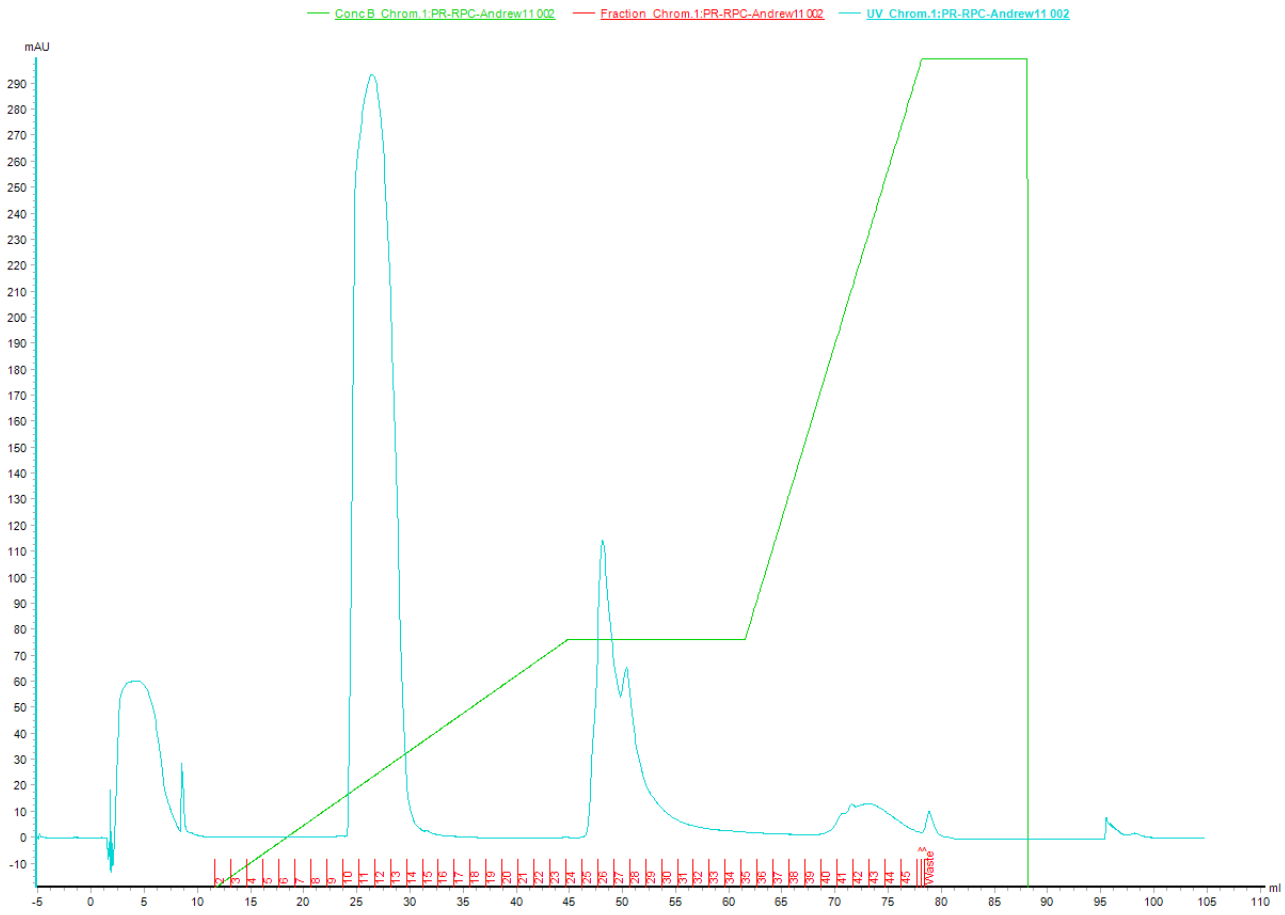

Figure 4.2 High performance liquid chromatogram of HIV protease.

4.1.3 Dialysis, refolding, and concentration of HIV-1 PR

HIV-1 PR was dialyzed and subsequently refolded by placing it in a solution of acetic acid at its active pH, 5.0, for ~4 hours. The protein was concentrated by centrifuging, and the

concentration was determined to be 8.4 mg/mL based on its absorbance at 280 nm. The HIV-1 PR was determined to be active via a fluorescence activity assay that involves cleaving of an artificial peptide substrate (of which the fluorescence is otherwise quenched).

4.2 Crystallization and data collection

4.2.1 Crystal optimization

After analyzing X-ray diffraction patterns from various crystals, it was determined that the crystal grown under the following conditions produced the highest resolution diffraction pattern: 0.1 M sodium cacodylate pH 6.0, 0.2 M magnesium acetate, and 16% PEG 8000.

4.2.2 X-ray diffraction

The crystal with the highest resolution diffraction diffracted at 1.09 Å and belonged to the space group $P2_12_12$. The diffraction pattern of this crystal was clean and well defined and was used to successfully determine the structure of HIV-1 PR in complex with ATV. The data collection statistics are summarized in Table 2.

Space group	$P2_12_12$
Unit cell dimensions (Å)	
α	58.72
β	85.79
γ	46.58
Resolution range (Å)	50-1.09 (1.13-1.09)
Unique reflections	91524 (5026)
R_{merge} (%)	7.8 (29.6)

I/σ (I)	28.1 (3.3)
Completeness (%)	92.9 (51.6)
Redundancy	6.4 (2.3)
Refinement	
R (%)	14.7
R_{free} (%)	17.4
Solvent molecules (total occupancies)	269 (209.7)
	1 Cl^- + 2 GOL + 1 CAC + 251 H_2O
RMS deviation from ideality	
Bonds (Å)	0.0153
Angle distance (Å)	0.0350
Average B-factors ($Å^2$)	
Wilson Plot B factor	7.9
Main-chain atoms	10.9
Side-chain atoms	16.2
Whole chain atoms	13.5
ATV	9.9
Solvent	23.8
RMS deviation to DRV (2IEN) (Å)	0.29

Table 2. X-ray diffraction data-collection and model-refinement statistics.

4.3 Analysis of HIV-1 atazanavir complex structure

The crystallography asymmetric units contain a HIV-1 PR dimer with the residues of the subunits numbered 1-99 and 100-199. Excellent electron density was shown for all protease atoms, ATV and solvent molecules.

4.3.1 RMSD between HIV-1 PR atazanavir complex and darunavir complex

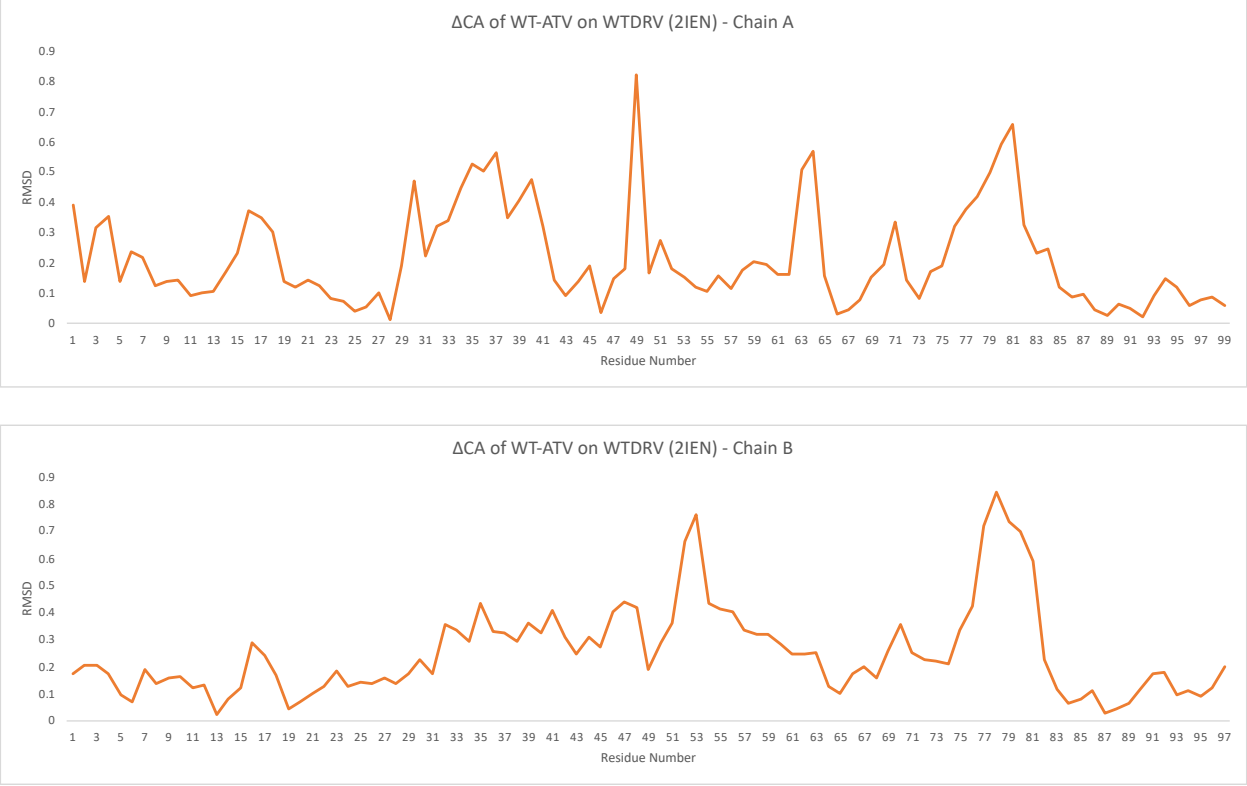

Figure 4.3. RMSD between WT HIV-1 PR in complex with atazanavir and WT HIV-1 PR in complex with darunavir.

Root-mean-square deviation (RMSD) values between WT HIV-1 PR in complex with ATV and WT HIV-1 PR in complex with DRV for chain A are displayed in the top, and RMSD values for chain B are displayed on the bottom.

4.3.2 Alternate conformations

Alternate conformations were modeled for 19 residues (Chain A – K7, E21, K45, I50, G51, I63, A71, V82, I84, L97 Chain B – K114, V132, S137, M146, I150, G151, Q161, E165, L197) in the crystal structure, as well as two conformations of atazanavir (Figure 4.7). The relative occupancy of the ATV conformations is 0.70/0.30. The residues with alternate conformations were not the same in both subunits, aside from I50/I150, G51/G151 and L97/L197, in which alternate conformations were modeled for both subunits (Figures 4.5 and 4.6). Clear electron density for was present for both conformations of the residues. $2F_0$-F_c electron density maps were used for all comparisons and all σ levels are set to 1.50 for each map in Figures 4.4-4.8.

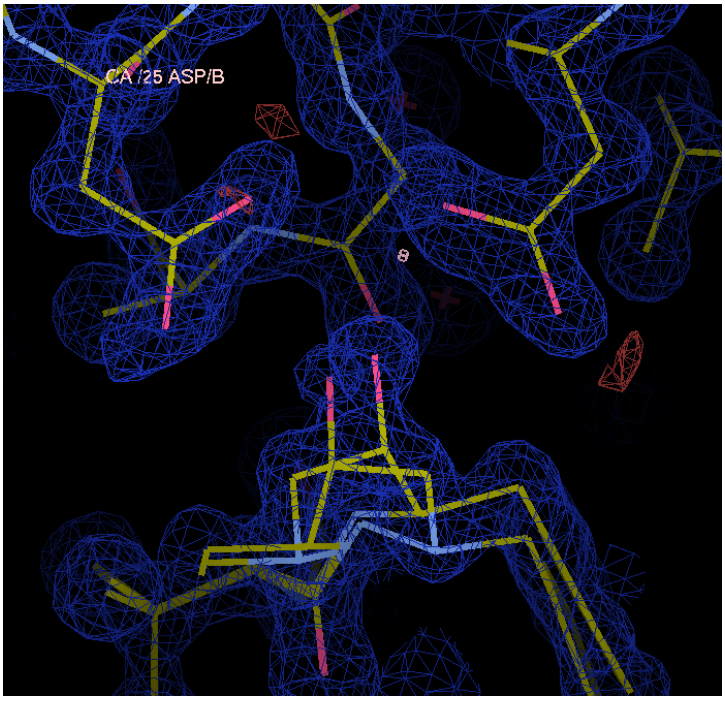

Figure 4.4 Electron density map of active site aspartates interacting with ATV

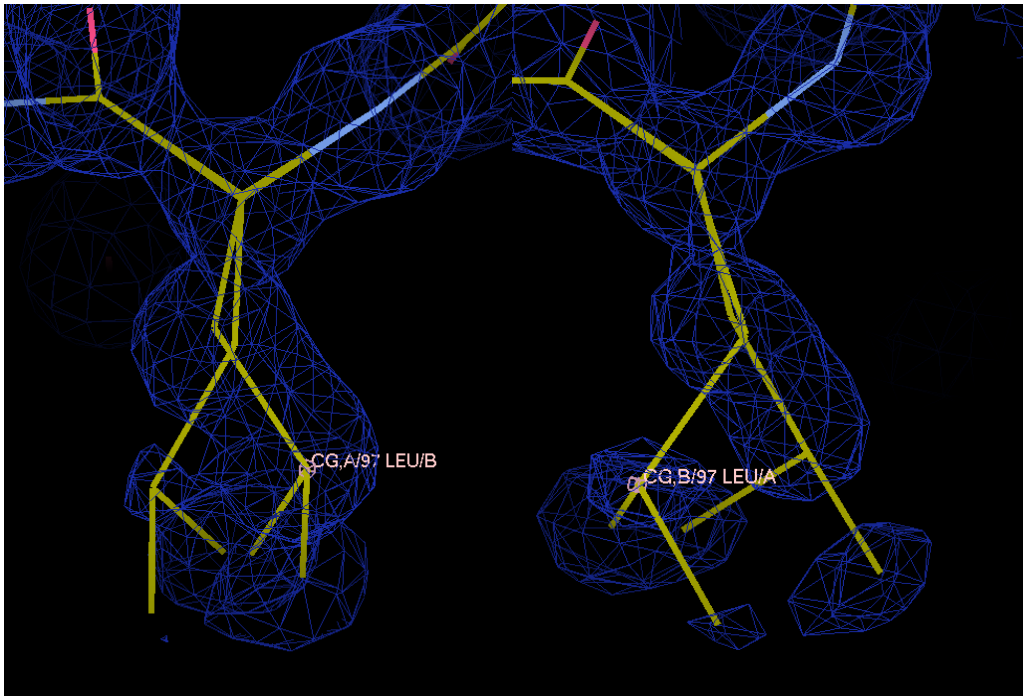

Figure 4.5 Electron density map displaying multiple conformations of L97 (left) and L197 (right)

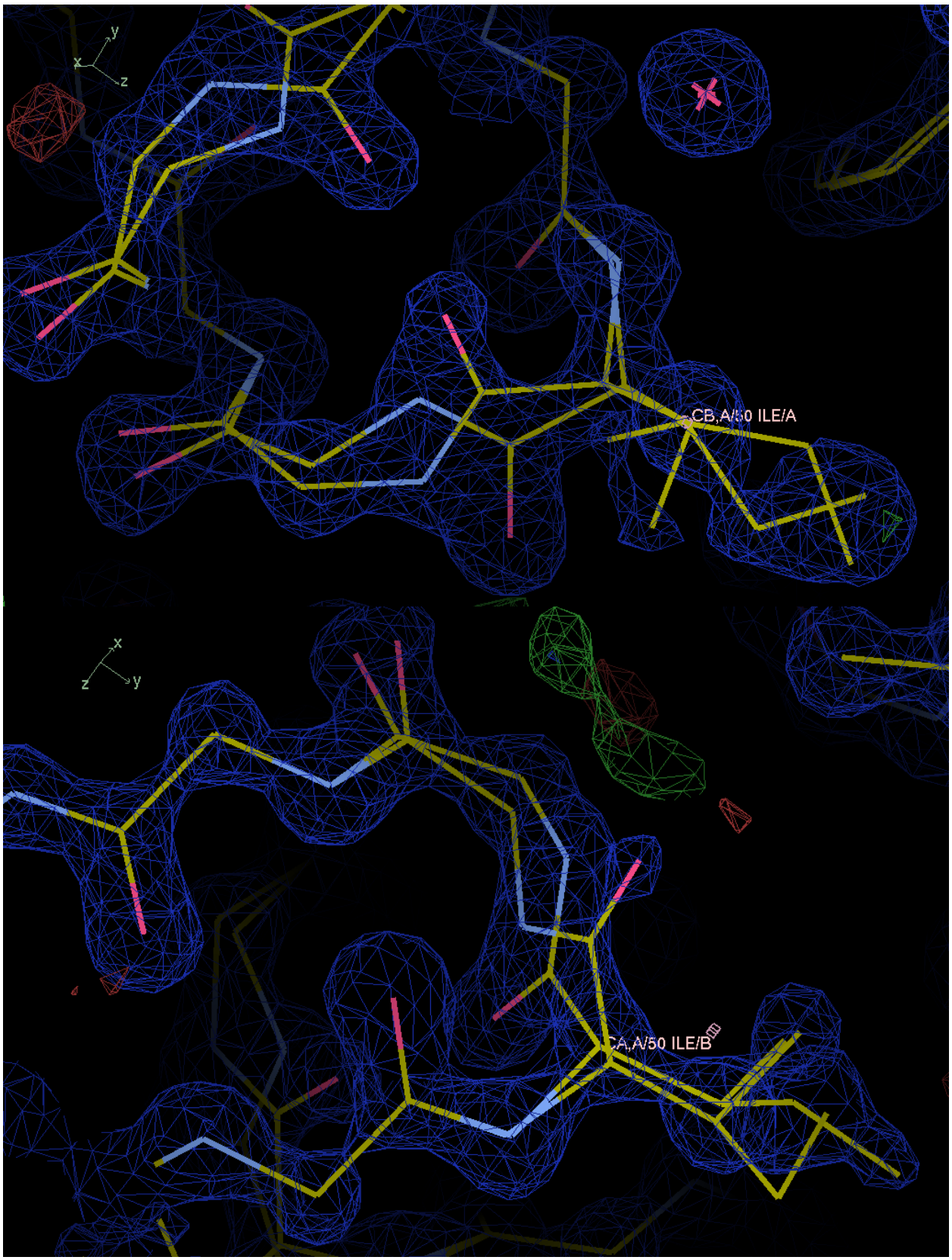

Figure 4.6 Alternate conformations of I50 and G51 (top) and I150 and G151 (bottom)

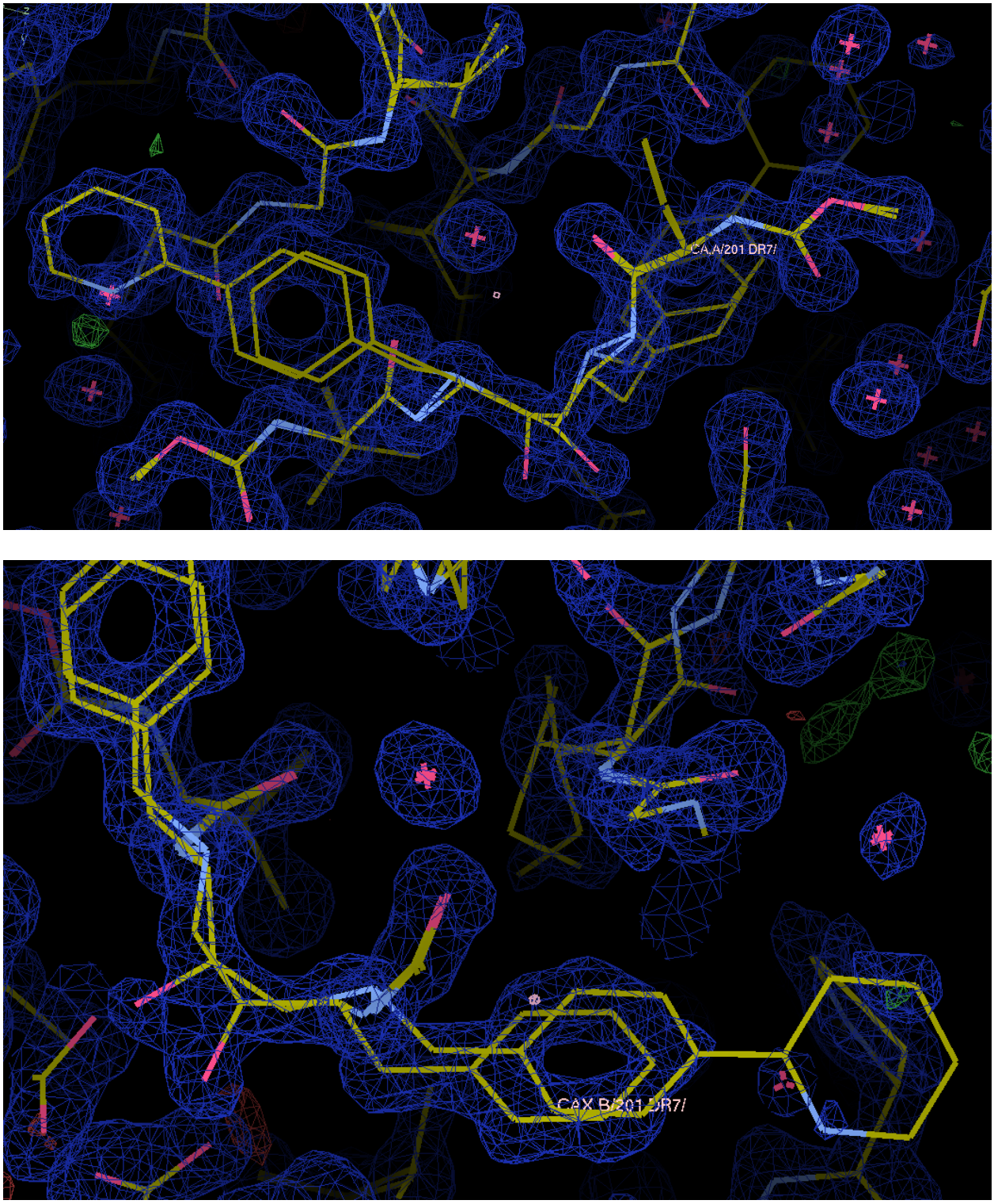

Figure 4.7 Electron density map displaying multiple atazanavir conformations

4.3.3 Solvent structures

The high quality data allowed for modeling of a second shell of solvent, with over 200 water molecules included in the model, some with partial occupancy. Additionally, chloride was modeled, and glycerol and cacodylate were fitted to the density (examples are shown in Figure 4.8).

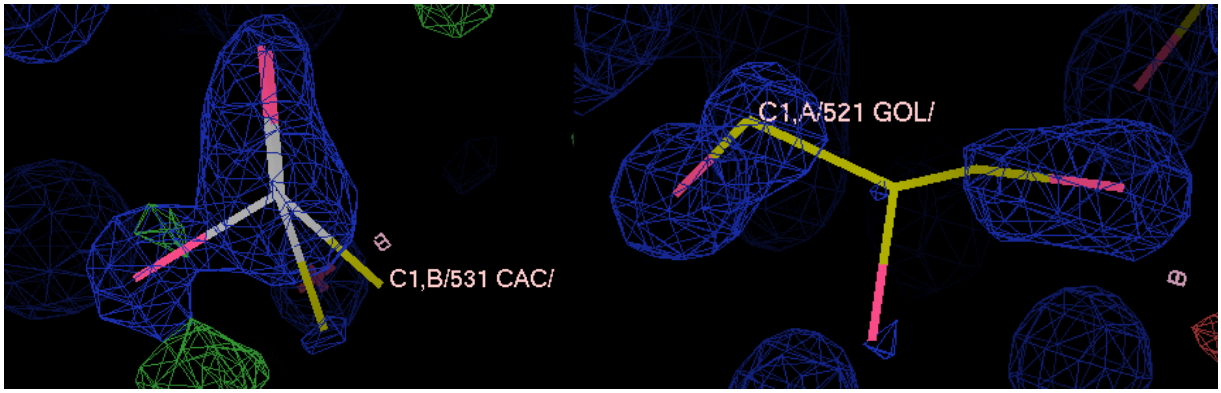

Figure 4.8 Electron density map of cacodylate (left) and glycerol (right)

4.4 Comparison of multiple conformations with published structures

2AQU modeled multiple conformations for K43, I47, I64, and ATV; 2AQU also reported 0.50 occupancy of I15, however no second conformation. Aside from ATV, none of these alternate conformations are the same as in the Weber WT structure.

3EL1 modeled multiple conformations for M46, I50, G51, V75, C95, I150, G151, C167, and ATV. M46, I50, G51, I150, and ATV also had multiple conformations in the Weber WT structure. However, V75, C95, and C167 did not exhibit multiple conformations in the Weber WT structure.

4.5 Comparison of atazanavir density with published structures

The ATV ligands from 3EL1 and 2AQU were superimposed with the ATV of the Weber WT HIV-1 PR in complex with ATV structure. 3EK1 was not used for comparisons, as it was published in conjunction with 3EL1. It is the same space group ($P2_12_12_1$) but displays one

conformation of ATV, rather than two like all of the other structures. Additionally, 3EL1 is slightly higher resolution than 3EKY (1.7 and 1.8 Å respectively), and the electron density map is clearly higher quality than 3EKY.

The ATV from the Weber WT structure is displayed in green, 3EL1 in pink, and 2AQU in teal. The superimposition of ATV shows that the ATV conformation modeled in 3EL1 differs fairly significantly from that of 2AQU and the Weber WT structure.

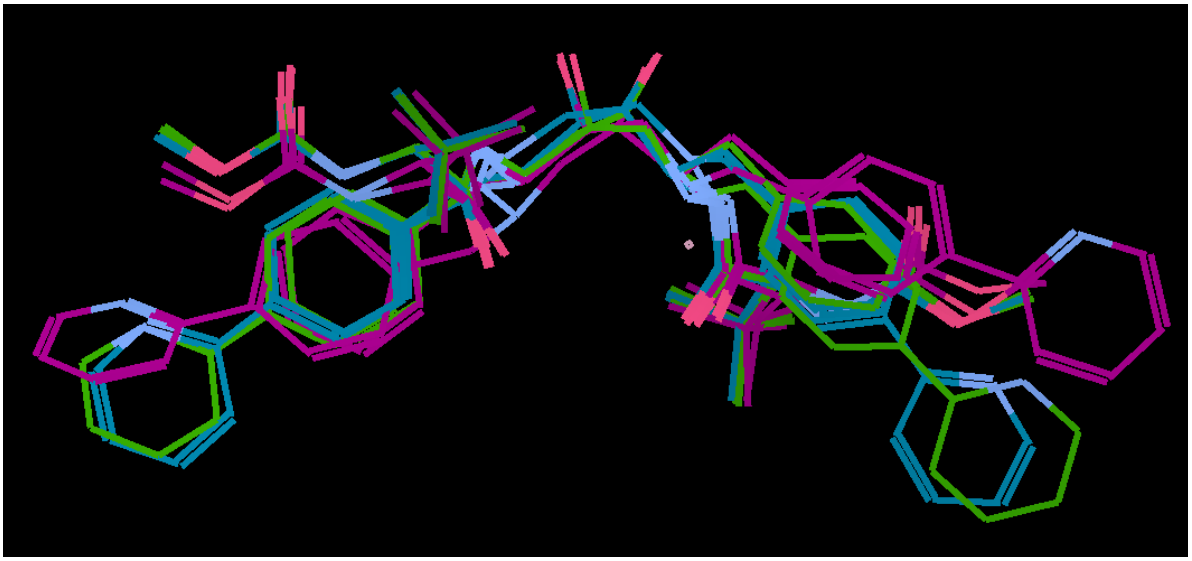

Figure 4.9 Superimposition of atazanavir of 2AQU, 3EL1 and Weber WT structure

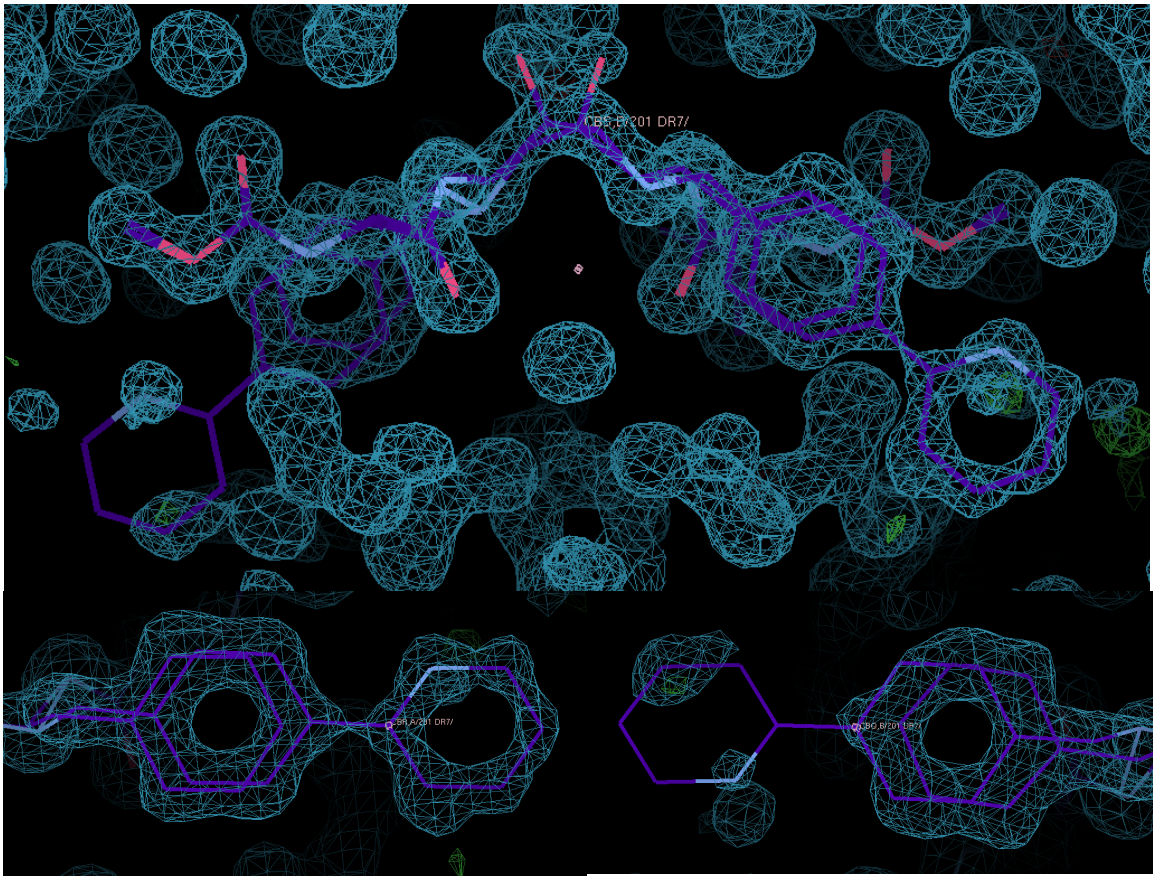

Figure 4.10 Electron density map of ATV from Weber WT structure

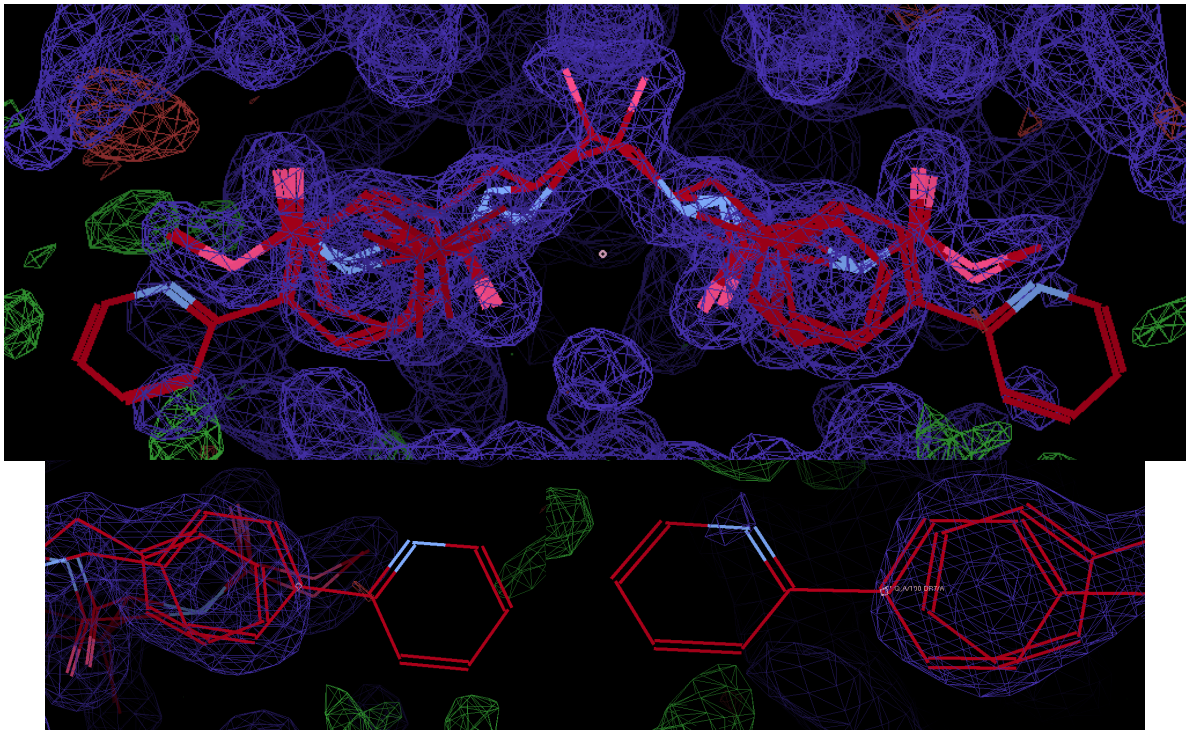

Figure 4.11 Electron density map of ATV from 3EL1.

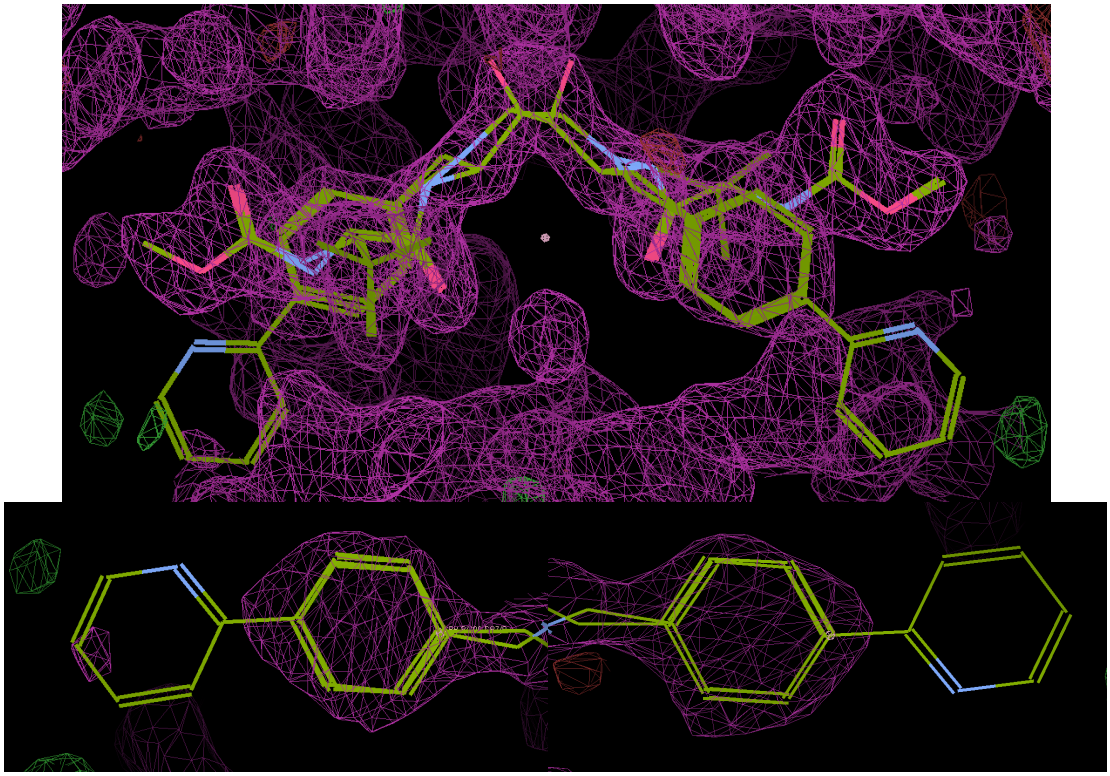

Figure 4.12 Electron density map of ATV from 2AQU

$2F_0$-F_c electron density maps were used and all σ levels are set to 1.50 for each map in Figures 4.10-12. 2AQU and 3EL1 have also modeled alternate conformations of ATV; however, the occupancy of each conformation is 0.50/0.50 in each structure, whereas in the Weber WT structure, the occupancy is 0.70/0.30. The higher resolution Weber WT structure displays clear density for the major conformation of ATV and slightly less well-defined density for the minor conformation of ATV (Figure 4.10). Both 2AQU and 3EL1 show nearly no electron density for the terminal rings of ATV as seen in Figures 4.11 and 4.12.

4.6 Comparison of protease-inhibitor interactions

Protease-inhibitor interactions were compared between the ATV complex, and a previously reported DRV complex (PDB ID: 2IEN).[55] For both structures inhibitor was modeled in two conformations. However, when comparing the structures, only the major conformation was considered. The relative occupancy in the ATV complex is 0.70/0.30, and the relative occupancy of the DRV complex is 0.55/0.45. Hydrogen bonds between inhibitor and protease or solvent are demonstrated in Figure 4.15 and Figure 4.16.

The major conformation of ATV forms hydrogen bonds with the side chains of D25, D125, and D129 and the backbone of D29, G27, G127, and G148, as well as numerous waters. The major conformation of DRV forms hydrogen bonds with the side chains of D25, D30, and D125 and the backbone of G127, D129, and D130, in addition to waters. While ATV forms hydrogen bonds with the N in the amide of the D129 backbone, it does not form hydrogen bonds with D130, which attributes to the high barrier of resistance displayed by DRV.[42]

4.6.1 Hydrogen bonding comparison between HIV-1 PR atazanavir complex and darunavir complex

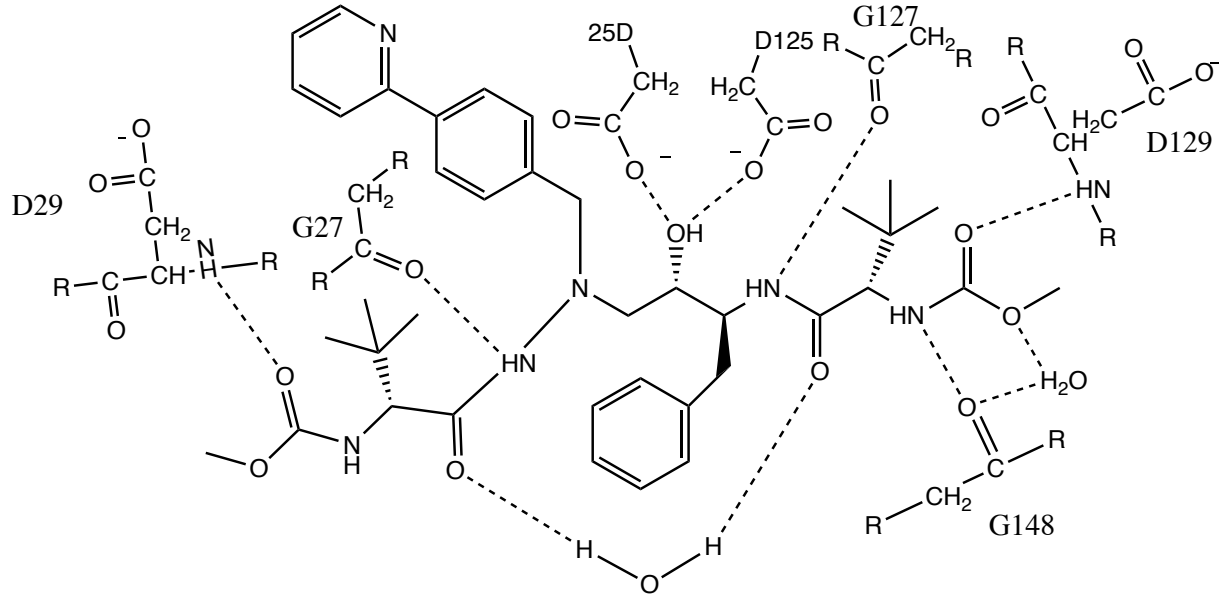

Figure 4.13 Interactions between ATV and HIV-1 PR, drawn in ChemDraw.

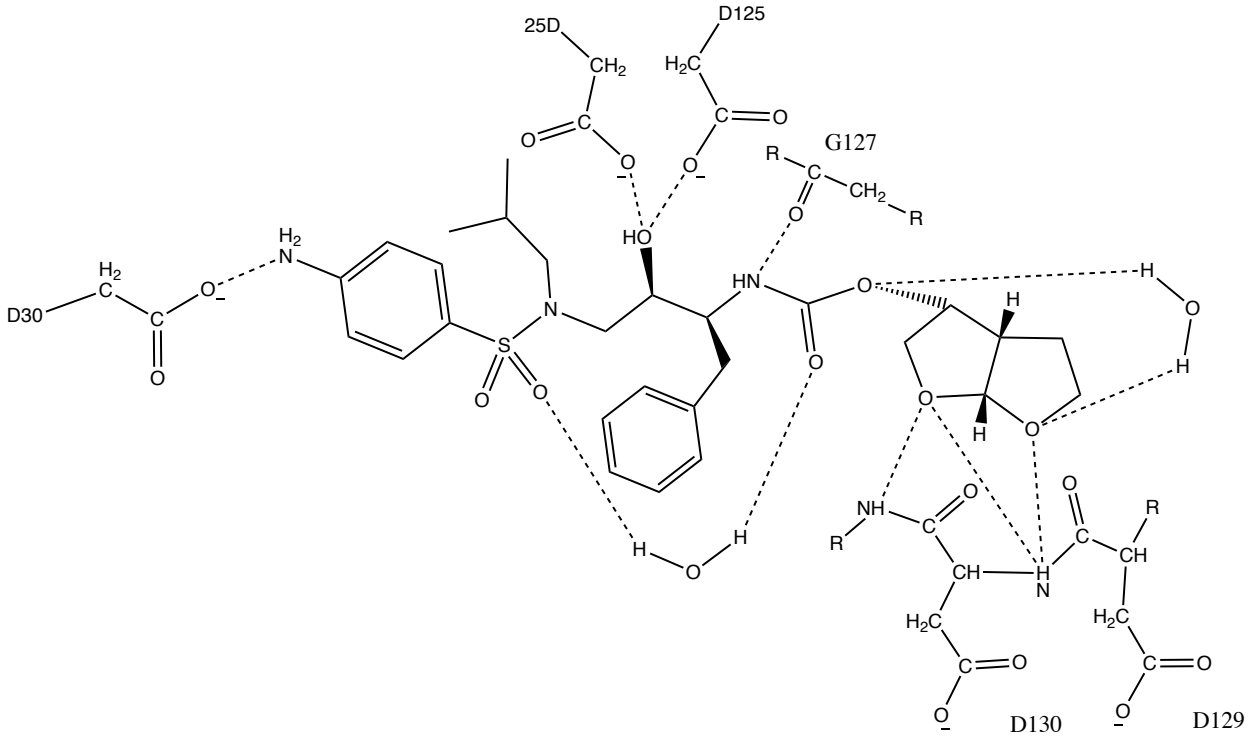

Figure 4.14 Interactions between DRV and HIV-1 PR, drawn in ChemDraw.

5 CONCLUSIONS

WT HIV-1 PR was expressed in inclusion bodies in *E. coli*, and purified using gel filtration chromatography and HPLC. The PR was then dialyzed, refolded, and concentrated by centrifugation, and then the protein was determined to be active using an enzymatic assay with an artificial peptide substrate. WT HIV-1 PR in complex with ATV was crystallized, and crystallization conditions producing the highest resolution diffraction patterns were determined to be: 0.1 M sodium cacodylate pH 6.0, 0.2 M magnesium acetate, and 16% PEG 8000. The structure of the WT HIV-1 PR in complex with ATV structure was solved with a resolution of 1.09 Å. Multiple conformations of 19 side chains were modeled. The structure indicates that ATV forms hydrogen bonds with three side chains and four hydrogen bonds with the PR backbone. Additionally, the high quality electron density map allowed for two conformations of ATV to be modeled (with occupancies of 0.70/0.30). This atomic resolution structure of HIV-1 PR in complex with ATV can be used to make comparisons of future crystal structures of highly drug resistant mutants in complex with atazanavir to provide insights to mechanisms of drug resistance, as well as provide insight to create new protease inhibitors with high barriers to resistance.

REFERENCES

1. Hemelaar, J., The origin and diversity of the HIV-1 pandemic. *Trends Mol Med* **2012,** *18* (3), 182-92.

2. Durack, D. T., Opportunistic infections and Kaposi's sarcoma in homosexual men. *N Engl J Med* **1981,** *305* (24), 1465-7.

3. Broder, S.; Gallo, R. C., A pathogenic retrovirus (HTLV-III) linked to AIDS. *N Engl J Med* **1984,** *311* (20), 1292-7.

4. Barre-Sinoussi, F.; Chermann, J.; Rey, F.; Nugeyre, M.; Chamaret, S.; Gruest, J.; Dauguet, C.; Axler-Blin, C.; Vezinet-Brun, F.; Rouzioux, C.; Rozenbaum, W.; Montagnier, L., Isolation of a T-lymphotropic retrovirus from a patient at risk for acquired immune deficiency syndrome (AIDS). *Science* **1983,** *220* (4599), 868-871.

5. Brandenberg, O. F.; Magnus, C.; Regoes, R. R.; Trkola, A., The HIV-1 Entry Process: A Stoichiometric View. *Trends Microbiol* **2015,** *23* (12), 763-774.

6. Hu, W. S.; Hughes, S. H., HIV-1 reverse transcription. *Cold Spring Harb Perspect Med* **2012,** *2* (10).

7. Lloyd, S. B.; Kent, S. J.; Winnall, W. R., The high cost of fidelity. *AIDS Res Hum Retroviruses* **2014,** *30* (1), 8-16.

8. Esposito, F.; Tramontano, E., Past and future. Current drugs targeting HIV-1 integrase and reverse transcriptase-associated ribonuclease H activity: single and dual active site inhibitors. *Antivir Chem Chemother* **2014,** *23* (4), 129-44.

9. Freed, E. O., HIV-1 assembly, release and maturation. *Nat Rev Microbiol* **2015,** *13* (8), 484-96.

10. Weber, I. T.; Kneller, D. W.; Wong-Sam, A., Highly resistant HIV-1 proteases and strategies for their inhibition. *Future Med Chem* **2015,** *7* (8), 1023-38.

11. Peters, B. S.; Conway, K., Therapy for HIV: past, present, and future. *Adv Dent Res* **2011,** *23* (1), 23-7.

12. Rachlis, A. R., Zidovudine (Retrovir) update. *CMAJ* **1990,** *143* (11), 1177-85.

13. Montaner, J. S. G.; Reiss, P.; Cooper, D.; Vella, S.; Harris, M.; Conway, B.; Wainberg, M. A.; Smith, D.; Robinson, P.; Hall, D.; Myers, M.; Lange, J. M. A.; for the, I. S. G., A Randomized, Double-blind Trial Comparing Combinations of Nevirapine, Didanosine, and Zidovudine for HIV-Infected Patients. *Jama* **1998,** *279* (12).

14. Gulick, R. M.; Mellors, J. W.; Havlir, D.; Eron, J. J.; Gonzalez, C.; McMahon, D.; Richman, D. D.; Valentine, F. T.; Jonas, L.; Meibohm, A.; Emini, E. A.; Chodakewitz, J. A., Treatment with indinavir, zidovudine, and lamivudine in adults with human immunodeficiency virus infection and prior antiretroviral therapy. *N Engl J Med* **1997,** *337* (11), 734-9.

15. Hogg, R. S.; Yip, B.; Kully, C.; Craib, K. J. P.; O'Shaughnessy, M. V.; Schechter, M. T.; Montaner, J. S. G., Improved survival among HIV-infected patients after initiation of triple-drug antiretroviral regimens. *Canadian Medical Association Journal* **1999,** *160* (5), 659-665.

16. Olding, M.; Enns, B.; Panagiotoglou, D.; Shoveller, J.; Harrigan, P. R.; Barrios, R.; Kerr, T.; Montaner, J. S. G.; Nosyk, B., A historical review of HIV prevention and care initiatives in British Columbia, Canada: 1996-2015. *J Int AIDS Soc* **2017,** *20* (1), 21941.

17. Croom, K. F.; Dhillon, S.; Keam, S. J., Atazanavir: a review of its use in the management of HIV-1 infection. *Drugs* **2009,** *69* (8), 1107-40.

18. Wensing, A. M.; van Maarseveen, N. M.; Nijhuis, M., Fifteen years of HIV Protease Inhibitors: raising the barrier to resistance. *Antiviral Res* **2010,** *85* (1), 59-74.

19. Titanji, B. K.; Aasa-Chapman, M.; Pillay, D.; Jolly, C., Protease inhibitors effectively block cell-to-cell spread of HIV-1 between T cells. *Retrovirology* **2013,** *10*, 161.

20. I.T., W.; R.W., H., Tackling the problem of HIV drug resistance. *Postępy Biochemii 62* (3), 273-279.

21. Louis, J. M.; Ishima, R.; Torchia, D. A.; Weber, I. T., HIV-1 protease: structure, dynamics, and inhibition. *Adv Pharmacol* **2007,** *55*, 261-98.

22. Erickson, J. W.; Burt, S. K., Structural mechanisms of HIV drug resistance. *Annu Rev Pharmacol Toxicol* **1996,** *36*, 545-71.

23. Shen, C. H.; Wang, Y. F.; Kovalevsky, A. Y.; Harrison, R. W.; Weber, I. T., Amprenavir complexes with HIV-1 protease and its drug-resistant mutants altering hydrophobic clusters. *FEBS J* **2010,** *277* (18), 3699-714.

24. Shen, C. H.; Chang, Y. C.; Agniswamy, J.; Harrison, R. W.; Weber, I. T., Conformational variation of an extreme drug resistant mutant of HIV protease. *J Mol Graph Model* **2015,** *62*, 87-96.

25. Shafer, R. W.; Schapiro, J. M., HIV-1 drug resistance mutations: an updated framework for the second decade of HAART. *AIDS Rev* **2008,** *10* (2), 67-84.

26. Wensing, A. M.; Calvez, V.; Gunthard, H. F.; Johnson, V. A.; Paredes, R.; Pillay, D.; Shafer, R. W.; Richman, D. D., 2017 Update of the Drug Resistance Mutations in HIV-1. *Top Antivir Med* **2017,** *24* (4), 132-133.

27. Lauring, A. S.; Frydman, J.; Andino, R., The role of mutational robustness in RNA virus evolution. *Nat Rev Microbiol* **2013,** *11* (5), 327-36.

28. Yin, L.; Liu, L.; Sun, Y.; Hou, W.; Lowe, A. C.; Gardner, B. P.; Salemi, M.; Williams, W. B.; Farmerie, W. G.; Sleasman, J. W.; Goodenow, M. M., High-resolution deep sequencing

reveals biodiversity, population structure, and persistence of HIV-1 quasispecies within host ecosystems. *Retrovirology* **2012,** *9*, 108.

29. Agniswamy, J.; Shen, C. H.; Aniana, A.; Sayer, J. M.; Louis, J. M.; Weber, I. T., HIV-1 protease with 20 mutations exhibits extreme resistance to clinical inhibitors through coordinated structural rearrangements. *Biochemistry* **2012,** *51* (13), 2819-28.

30. Agniswamy, J.; Louis, J. M.; Roche, J.; Harrison, R. W.; Weber, I. T., Structural Studies of a Rationally Selected Multi-Drug Resistant HIV-1 Protease Reveal Synergistic Effect of Distal Mutations on Flap Dynamics. *PLoS One* **2016,** *11* (12), e0168616.

31. Louis, J. M.; Deshmukh, L.; Sayer, J. M.; Aniana, A.; Clore, G. M., Mutations Proximal to Sites of Autoproteolysis and the alpha-Helix That Co-evolve under Drug Pressure Modulate the Autoprocessing and Vitality of HIV-1 Protease. *Biochemistry* **2015,** *54* (35), 5414-24.

32. Johnson, V. A.; Brun-Vezinet, F.; Clotet, B.; Gunthard, H. F.; Kuritzkes, D. R.; Pillay, D.; Schapiro, J. M.; Richman, D. D., Update of the drug resistance mutations in HIV-1: December 2010. *Top HIV Med* **2010,** *18* (5), 156-63.

33. Park, J. H.; Sayer, J. M.; Aniana, A.; Yu, X.; Weber, I. T.; Harrison, R. W.; Louis, J. M., Binding of Clinical Inhibitors to a Model Precursor of a Rationally Selected Multidrug Resistant HIV-1 Protease Is Significantly Weaker Than That to the Released Mature Enzyme. *Biochemistry* **2016,** *55* (16), 2390-400.

34. Zheng, H.; Handing, K. B.; Zimmerman, M. D.; Shabalin, I. G.; Almo, S. C.; Minor, W., X-ray crystallography over the past decade for novel drug discovery - where are we heading next? *Expert Opin Drug Discov* **2015,** *10* (9), 975-89.

35. Chen, J. C.; Hanson, B. L.; Fisher, S. Z.; Langan, P.; Kovalevsky, A. Y., Direct observation of hydrogen atom dynamics and interactions by ultrahigh resolution neutron protein crystallography. *Proc Natl Acad Sci U S A* **2012,** *109* (38), 15301-6.

36. Weber, I. T.; Waltman, M. J.; Mustyakimov, M.; Blakeley, M. P.; Keen, D. A.; Ghosh, A. K.; Langan, P.; Kovalevsky, A. Y., Joint X-ray/neutron crystallographic study of HIV-1 protease with clinical inhibitor amprenavir: insights for drug design. *J Med Chem* **2013,** *56* (13), 5631-5.

37. Binshtein, E.; Ohi, M. D., Cryo-electron microscopy and the amazing race to atomic resolution. *Biochemistry* **2015,** *54* (20), 3133-41.

38. Wang, G.; Zhang, Z. T.; Jiang, B.; Zhang, X.; Li, C.; Liu, M., Recent advances in protein NMR spectroscopy and their implications in protein therapeutics research. *Anal Bioanal Chem* **2014,** *406* (9-10), 2279-88.

39. Wlodawer, A.; Minor, W.; Dauter, Z.; Jaskolski, M., Protein crystallography for aspiring crystallographers or how to avoid pitfalls and traps in macromolecular structure determination. *FEBS J* **2013,** *280* (22), 5705-36.

40. Zheng, H.; Hou, J.; Zimmerman, M. D.; Wlodawer, A.; Minor, W., The future of crystallography in drug discovery. *Expert Opin Drug Discov* **2014,** *9* (2), 125-37.

41. Wlodawer, A., Rational approach to AIDS drug design through structural biology. *Annu Rev Med* **2002,** *53*, 595-614.

42. Ghosh, A. K.; Chapsal, B. D.; Weber, I. T.; Mitsuya, H., Design of HIV protease inhibitors targeting protein backbone: an effective strategy for combating drug resistance. *Acc Chem Res* **2008,** *41* (1), 78-86.

43. Luft, J. R.; Newman, J.; Snell, E. H., Crystallization screening: the influence of history on current practice. *Acta Crystallogr F Struct Biol Commun* **2014,** *70* (Pt 7), 835-53.

44. Jain, D.; Lamour, V., Computational tools in protein crystallography. *Methods Mol Biol* **2010,** *673*, 129-56.

45. MS, S.; JHJ, M., x Ray crystallography. *Molecular Pathology* **2000,** *53* (1), 8-14.

46. Bunkoczi, G.; Echols, N.; McCoy, A. J.; Oeffner, R. D.; Adams, P. D.; Read, R. J., Phaser.MRage: automated molecular replacement. *Acta Crystallogr D Biol Crystallogr* **2013,** *69* (Pt 11), 2276-86.

47. Wlodawer, A.; Minor, W.; Dauter, Z.; Jaskolski, M., Protein crystallography for non-crystallographers, or how to get the best (but not more) from published macromolecular structures. *FEBS J* **2008,** *275* (1), 1-21.

48. Clemente, J. C.; Coman, R. M.; Thiaville, M. M.; Janka, L. K.; Jeung, J. A.; Nukoolkarn, S.; Govindasamy, L.; Agbandje-McKenna, M.; McKenna, R.; Leelamanit, W.; Goodenow, M. M.; Dunn, B. M., Analysis of HIV-1 CRF_01 A/E protease inhibitor resistance: structural determinants for maintaining sensitivity and developing resistance to atazanavir. *Biochemistry* **2006,** *45* (17), 5468-77.

49. King, N. M.; Prabu-Jeyabalan, M.; Bandaranayake, R. M.; Nalam, M. N.; Nalivaika, E. A.; Ozen, A.; Haliloglu, T.; Yilmaz, N. K.; Schiffer, C. A., Extreme entropy-enthalpy compensation in a drug-resistant variant of HIV-1 protease. *ACS Chem Biol* **2012,** *7* (9), 1536-46.

50. McCoy, A. J.; Grosse-Kunstleve, R. W.; Adams, P. D.; Winn, M. D.; Storoni, L. C.; Read, R. J., Phaser crystallographic software. *J Appl Crystallogr* **2007,** *40* (Pt 4), 658-674.

51. Z., O.; W., M., Processing of X-ray diffraction data collected in oscillation mode. *Meth. Enzymol.* **1997,** *276*, 307-26.

52. Murshudov, G. N.; Vagin, A. A.; Dodson, E. J., Refinement of macromolecular structures by the maximum-likelihood method. *Acta Crystallogr D Biol Crystallogr* **1997,** *53* (Pt 3), 240-55.

53. Emsley, P.; Cowtan, K., Coot: model-building tools for molecular graphics. *Acta Crystallogr D Biol Crystallogr* **2004,** *60* (Pt 12 Pt 1), 2126-32.

54. Sheldrick, G. M., Crystal structure refinement with SHELXL. *Acta Crystallogr C Struct Chem* **2015,** *71* (Pt 1), 3-8.

55. Tie, Y.; Boross, P. I.; Wang, Y. F.; Gaddis, L.; Hussain, A. K.; Leshchenko, S.; Ghosh, A. K.; Louis, J. M.; Harrison, R. W.; Weber, I. T., High resolution crystal structures of HIV-1 protease with a potent non-peptide inhibitor (UIC-94017) active against multi-drug-resistant clinical strains. *J Mol Biol* **2004,** *338* (2), 341-52.